Lawrence Berkeley National Laboratory

Title

Transient structuring of liquids using dissipative interfacial assemblies

Permalink

Journal

ISSN

Authors

Gleeson, Sarah E

Fink, Zachary

Ashby, Paul D

et al.

Publication Date

DOI

Copyright Information

Peer reviewed

Transient Structuring of Liquids Using Dissipative Interfacial Assemblies

Sarah E. Gleeson[1], Paul D. Ashby[2], Thomas P. Russell[1,3,4], Brett A. Helms[1,2]*

Affiliations:

[1]Materials Sciences Division, Lawrence Berkeley National Laboratory, Berkeley, CA 94720 USA.

[2]The Molecular Foundry, Lawrence Berkeley National Laboratory, Berkeley, CA 94720 USA.

[3]Polymer Science and Engineering Department, University of Massachusetts, Amherst, MA

01003 USA.

[4]World Premier Institute–Advanced Institute for Materials Research, Tohoku University, Sendai

980-8577, Japan

 *Correspondence to: bahelms@lbl.gov.

ABSTRACT: Structured liquids stabilized by interfacial assemblies enable compartmentalization of reactive species and spatial control over chemical systems. To prescribe a lifetime for structured liquids would require that the assemblies, initially confined to the interface, eventually revert to molecularly dissolved species over time. Here, we show that structured liquids with programmable lifetimes can be created in an oil phase from water containing poly(acrylic acid) and a carbodiimide fuel, which transiently generate polymer aggregates that solidify at the interface. When the fuel is consumed, the assembly dissipates to re-form soluble polymer chains; the out-of-equilibrium structure imparted to the liquid is then lost. We exploit this phenomenon for controlled coalescence and further demonstrate that liquid compartment lifetimes are readily extended by re-fueling the system. Using interfacial rheology, we identify crossover points in the interfacial storage and loss moduli at times commensurate with the amount of fuel, evidencing transitions between solid- like and liquid-like assemblies that cause the compartmentalized liquids to burst. This work opens the door to time- and shape-programmable chemical systems.
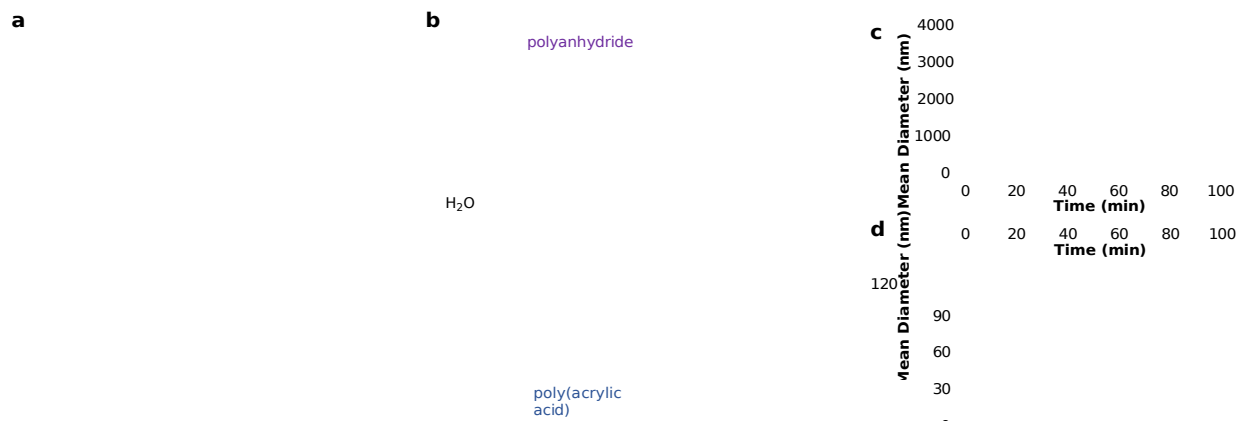
Main Text:

Compartmentalization is used in Nature to separate and protect biochemical processes, often utilizing liquid–liquid phase separation or lipid membranes.[1,2] This can be mimicked with structured liquids that energetically trap colloids or surfactants at the interface between immiscible liquids, creating shape-programmable compartments for confining functional chemistries in space.[3-9] Programming transience in structured liquids remains a challenge, yet

would enable autonomous control over a broad range of synthetic and biomimetic chemical systems. While external stimuli have been used to disrupt surfactant binding and reshape liquid interfaces,[10-15]

there are, yet, no time-programmable structured liquids. An ideal solution for programming autonomous structural changes would involve the desorption of colloids or surfactants from the interface at a predetermined time, such that the compartmentalized liquid phase could release its contents to its surroundings.

Here, we show that by creating fueled surfactants to form a transient interfacial assembly, we can design structured liquids with programmable lifetimes (**Fig. 1a**). We use a chemical fuel to enable dissipative self-assembly (DSA) at a liquid–liquid interface, a process inspired by natural systems that rely on chemical energy to form dynamic structures with unique properties.[16-23] In our system, chemical fuel converts soluble polymer chains into dispersed colloids, which densely pack at the interface. The interface jams with energetically trapped surfactants, locking the interfacial geometry in place. The jammed state relies on the continued consumption of chemical fuel: when the fuel expires, hydrolysis of the surfactant leads to unjamming and thereafter desorption.

a   **b**

polyanhydride

H$_2$O

poly(acrylic acid)

c

Mean Diameter (nm)

4000
3000
2000
1000
0

0   20   40   60   80   100
         Time (min)

d

0   20   40   60   80   100
         Time (min)

Mean Diameter (nm)

120
90
60
30
0

Fig. 1. Structuring liquids using transient interface-active polymer colloids. a, Scheme showing the DSA cycle converting soluble polymer chains into an interfacial assembly using EDC as a chemical fuel. **b,** EDC fuels conversion of polymeric carboxylic acids to anhydrides on a PAA chain, and hydrolysis reverts anhydrides into carboxylic acids. **c,** DLS of EDC-fueled PAA in aqueous solution for different fuel concentrations. Each data point is an average of three independent measurements. **d,** Data shown in panel **c**, but scaled to show smaller-diameter colloids.

By approaching surfactant jamming as an out-of-equilibrium condition rather than an energetic endpoint, we can engineer and control liquid systems with well-defined lifetimes. In this way, time-programmable structured liquids are complementary to other dissipative functional materials, including molecular rotors,[24,25] self-erasing inks,[26,27] time-programmable release vessels,[28,29] and transient chemical reactors.[30,31] However, no prior system has employed dissipative energy to control behavior of molecules at an interface, or to use chemical fuel to

spatially control the architectures of immiscible liquid compartments. Our approach utilizes hierarchical levels of

dissipative assembly: fueled chemical changes lead to assembly into polymer colloids that form transient interfacial films. This enables the generation of hierarchical systems of liquids with lifetimes determined by dissipative disruption of surfactant jamming.

Results and Discussion

To program an internal clock into a structured liquid, we use a carbodiimide condensation reagent as a chemical fuel (**Fig. 1a,b**). The fuel, 1-ethyl-3-(3-dimethylaminopropyl)carbodiimide hydrochloride (EDC), reacts with hydrophilic and solubilizing carboxylic acid pendants on poly(acrylic acid) (PAA) to create hydrophobic and de-solubilizing cyclic anhydrides and increase the polymer's affinity for an oil–water interface (**Fig. 1b**). **Fig. 1b** shows the formation of intra- chain anhydrides, but inter-chain linkages may also form, especially if aggregation or interfacial confinement leads to chains being in close proximity. As EDC reacts, it is converted to waste urea (EDU). The fuel supply dwindles over time, allowing the interfacial assembly to have a finite lifetime based on competing rates of anhydride formation and hydrolysis. This temporally controlled interfacial assembly allows for autonomous modulation of interfacial structure and properties, resulting in liquid systems with compositions defined not only in space by compartmentalization, but also in time by energy dissipation.

Conformational changes of PAA in response to EDC are important to understanding its interfacial behavior, since colloidal particles screen the interfacial energy with a magnitude that scales with the square of the colloid radius, energetically trapping colloids above a certain size at

the interface.[32] We used dynamic light scattering (DLS) to show that EDC-fueled PAA not only

forms

colloids in aqueous solution, but that their size and lifetime is directly dependent on the fuel concentration. Upon fueling with 10 mM and 15 mM EDC, micrometer-diameter aggregates form and then dissipate (**Fig. 1c**). For 7.5 mM EDC, only a small change in the hydrodynamic diameter was measured (**Fig. 1d**); no change was seen for 5 mM EDC relative to unfueled PAA.

PAA adsorption and desorption from the interface was tracked by measuring changes in interfacial tension (*IFT*). Pendant drop tensiometry was used to measure *IFT* over time for an oil–water interface composed of toluene against a buffered aqueous solution (pH 6) of 0.1 w/v% PAA fueled with 10 mM EDC (**Fig. 2a**). *IFT* drops rapidly as polymer adsorbs to the toluene–water interface, reducing the high-energy interfacial area. Within minutes, the *IFT* plateaus at 16.3 mN m^{-1} as the interfacial material reaches an equilibrium areal density. Beginning 45 minutes after fueling, polymer autonomously desorbs from the interface and *IFT* increases steadily to a second plateau at ~28.9 mN m^{-1}. This higher-*IFT* plateau is stable for more than 8 h, indicating this is the final equilibrium state (**Supplementary Fig. 1**). Interestingly, prior to polymer desorption there is a dip in *IFT*, which we attribute to the onset of anhydride hydrolysis allowing for reconfiguration and denser packing of polymers at the interface. **Supplementary Fig. 2** shows control tensiometry measurements with each component individually, confirming that neither PAA nor EDC alone demonstrates the cyclic *IFT* behavior of polymer and fuel together.
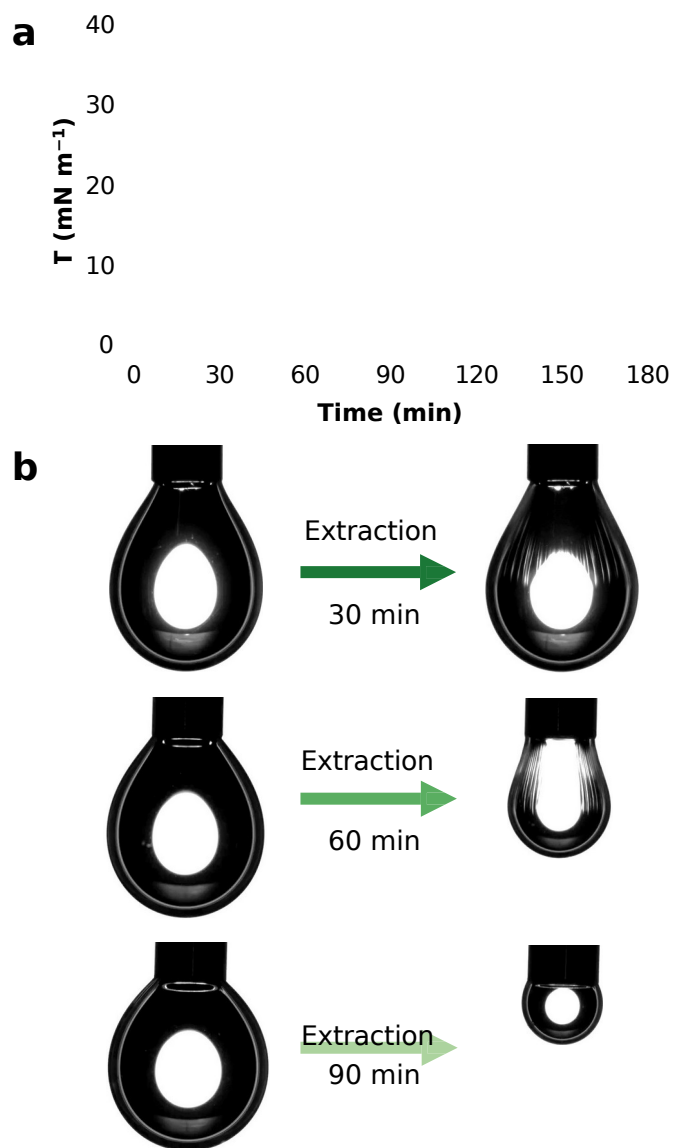
Fig. 2. Dissipative self-assembly of polymer films at a liquid–liquid interface promoted by a chemical fuel. a, *IFT* over time, as measured by pendant drop tensiometry, for a toluene–water interface with PAA and 10 mM EDC in the buffered water drop. Time 0 is when EDC and PAA are mixed. Inset picture shows an image of a pendant drop with each component labeled. **b,**

Images

of pendant drops with the same composition as panel **a** at different times. Left-hand images are the drops before extraction, and right-hand images are drops shortly after the onset of interface wrinkling, if observed. Each extraction time point is shown with arrows on the plot in panel **a**.

Changes in *IFT* over time reflect changes in the jammed state of the interfacial film. Pendant drops of aqueous-fueled PAA were formed in toluene and aspirated at different times (**Fig. 2b and Supplementary Video 1**). After 30 minutes, when the interfacial system is at its *IFT*-minimum plateau, the surface of the drop wrinkles with very little extracted volume. This is a jammed interfacial assembly, meaning that slight compression of the interfacial area leads to buckling of the film rather than desorption. Extraction after 60 minutes requires a greater reduction in interfacial area to see wrinkling, due to the lower areal density of trapped material. After 90 minutes, the surface of the droplet no longer behaves as a solid when compressed, indicating that the final equilibrium state of the assembly is unjammed. **Supplementary Fig. 3 and Supplementary Video 1** show that unfueled PAA alone is not jammed at the interface, and therefore we have demonstrated a full jamming–unjamming DSA cycle, with fuel causing jamming and unjamming autonomously.

Tuning the Lifetime of the Fueled Assembly

The ability to adjust the internal clock of a structured liquid is crucial for temporal control over compartmentalization. Previous studies for EDC-fueled DSA have shown that the concentration of fuel determines the lifetime of the out-of-equilibrium assemblies,[33,34] but how fuel impacts the

absorption and desorption at an interface is yet unstudied. Assembly at an oil–water interface

offers

insight into how the DSA cycle is impacted for a structure where fueling and hydrolysis can only occur on one side of the assembly.

We varied the concentration of EDC added to the aqueous phase and found that the jammed plateau becomes longer as more EDC is present (**Fig. 3a**). For 0.1 w/v% PAA, 5 mM EDC was too low to reach the same minimum *IFT* as the higher fuel concentrations, possibly due to a lower extent of anhydride formation or a rapid exhaustion of fuel. However, 5 mM EDC was sufficient to initially decrease *IFT*, showing that a fuel concentration too low for colloid formation (**Fig. 1d**) can still drive small polymer surfactants or aggregates to the interface. The formation of insoluble aggregates at higher fuel concentrations is concomitant with a transient but stable interfacial film with low *IFT* and wrinkling upon compression of the interface. A lower minimum *IFT* is reached using 7.5 mM EDC than higher concentrations, likely due to the formation of nano-sized rather than micron-sized aggregates, which can pack more densely at the interface (**Fig. 1c,d**). All concentrations of EDC tested result in a lower *IFT* value for the final state than the control with no EDC, suggesting that some polymer becomes irreversibly trapped at the interface, either due to incomplete hydrolysis or the formation of *N*-acyl urea on the polymer chain. However, none of the EDC concentrations tested exhibited jamming after 180 minutes.

a

b
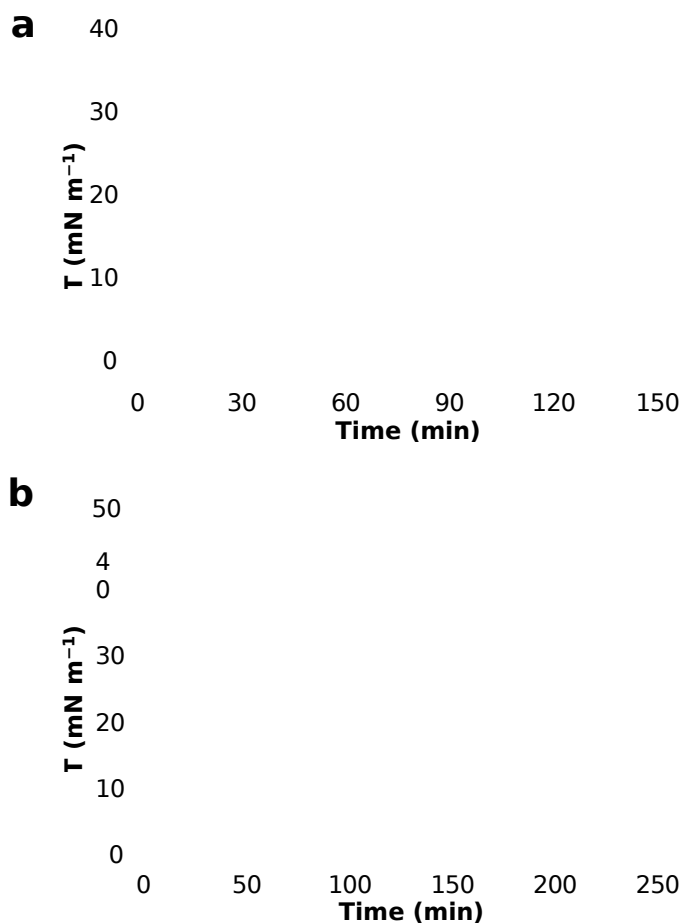
Fig. 3. Prescribing and sustaining the lifetime of interfacial films used to transiently structure liquids. (a) IFT over time for a toluene–water/PAA interface with different concentrations of fuel added. The data represent the average of three independent trials; the shaded region is one standard deviation above and below average. **(b)** IFT over time for a dodecane–water/PAA interface with EDC added at 20, 80, 140, and 200 minutes (indicated with arrows). Inset shows an image of an inverted pendant drop.

The ability to make *in-situ* adjustments to the interfacial structure allows for a more responsive and reconfigurable system. To this end, we demonstrate that the system can be repeatedly re-fueled to create cycles of jamming and unjamming (**Fig. 3b**). We performed tensiometry on an inverse dodecane pendant drop surrounded by aqueous PAA and added EDC for a total of four fueling cycles. Each time fuel was added there was a drop in the *IFT* before the system recovered, but with each consecutive cycle, the upper and lower *IFT* values decreased as did the duration of the jammed plateau. This could be due to accumulation of irreversibly adsorbed polymer, accumulation of EDU waste over time, or dilution of the polymer with each subsequent addition of aqueous EDC solution.

Rheology of fueled surfactant at a liquid–liquid interface

Having shown that EDC-fueled PAA forms a jammed interfacial film, the mechanical properties of this assembly over time were tested using a Du Noüy ring placed at a planar water–silicone oil interface within a double-wall channel (**Fig. 4**). For all concentrations of EDC (5, 7.5, or 10 mM), a solid-like layer formed with the interfacial storage modulus (G_i') exceeding the interfacial loss modulus (G_i''). Interfaces fueled with 10 mM and 7.5 mM EDC show similar behavior with different timing: an initial G_i' plateau of ~1.8×10^2 Pa·m as the solid-like film is stable followed by a drop-off of 4 orders of magnitude as the film dissipates. The same films have G_i'' initially decreasing by ~1 Pa·m, then increasing by ~10 Pa·m before dropping below the instrument detection limit. We hypothesize that the loss moduli initially decrease as the films continue to densify, limiting locations of slip in the film. Initial hydrolysis of the assembly

reopens these slip locations, increasing the film viscosity. Continued hydrolysis leads to desorption and complete

loss of integrity of the film, giving a low-viscosity liquid-like character. The interface structured

with 5 mM EDC does not show the same behavior, with both storage and loss moduli dropping

off quickly after measurements were taken, which is consistent with the *IFT* results for this fuel

concentration (**Fig. 3a**). Interestingly, crossover points across all EDC concentrations tested fell

within a similar range (3.5–6.0 Pa·m) and the peak G_i'' before dissipation was ~20 Pa·m for all

samples, evidencing consistent transitions between solid-like and liquid-like assemblies.
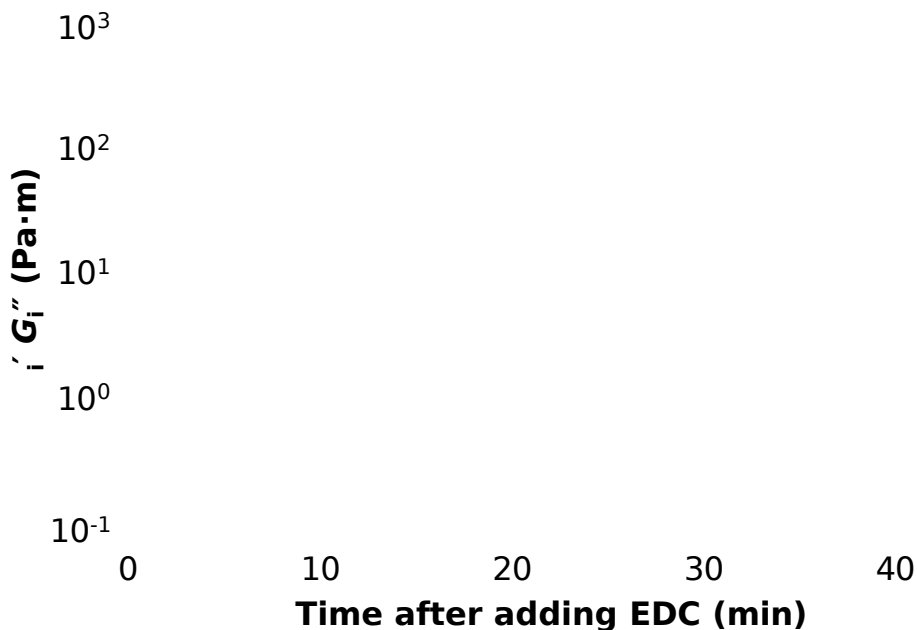
Fig. 4. *In-situ* **characterization of solid–liquid phase transformations in chemically-fueled**

interfacial polymer assemblies. Interfacial storage (G_i', blue circles) and loss (G_i'', orange

diamonds) moduli over time for 5, 7.5, and 10 mM EDC. Time 0 is when EDC and PAA are

mixed. The interface is silicone oil against buffered water (pH 6) containing 0.1 w/v% PAA and

EDC.

Temporal control over compartment coalescence

Transient mechanical stability of interfacial films has promising applications for temporally controlled segregation of liquids. We demonstrated this by creating microfluidic droplets of silicone oil surrounded by aqueous EDC-fueled PAA (**Fig. 5a**). As the fueled polymer migrates to the oil–water interface, the interface becomes stabilized against coalescence of the oil droplets for a time determined by the fuel concentration (**Fig. 5b,c**). Fueling with 10 mM EDC results in oil droplets that retain close to 100% of their initial number until a rapid drop-off centered around 55 minutes. The droplet lifetime decreases as the fuel concentration decreases, although droplets show the same behavior of stability followed by rapid dissipation. When the droplet temporal stability is compared to the *IFT* profile over time for a water–silicone oil interface (**Supplementary Fig. 4**), the time when 50% of droplets remain corresponds to the time when the *IFT* has increased slightly, with enough polymer desorbing for the interface to weaken and the droplets to rupture. If no EDC is present when forming the droplets (**Supplementary Fig. 5**), very few droplets are deposited since most coalesce while in the microfluidic device, or before the first image can be captured.

We also demonstrate that adding further fuel to a jammed interfacial assembly can extend the lifetime of the structured liquid. Microfluidic drops were fueled with 10 mM EDC, and, before the expected coalescence time of the droplets, we added an additional 7.5 mM EDC. This was repeated 3 times total, and the droplet numbers over time are plotted in **Fig. 5d**. Multiple additions of fuel leads to stabilization of droplets well beyond the lifetime from a single fueling event. With three additions of fuel every 40 minutes, approximately 50% of droplets were still

present after 3 hours.

While droplet losses occurred with each addition due to mechanical perturbation during refueling, it is promising that the lifetime of the jammed interface can be adjusted in real time.

a

b

c
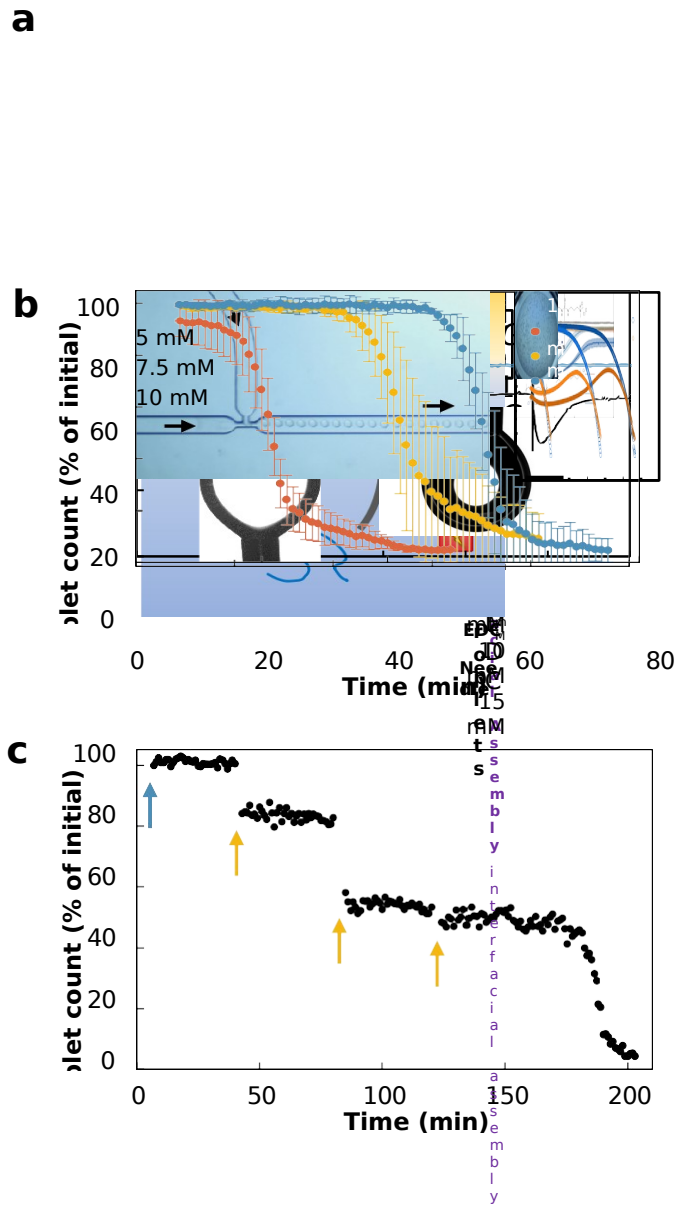
Fig. 5. Time-programmable structured liquids for controlling droplet coalescence. a, Optical microscope image of the microfluidic T-junction for making oil-in-water droplets. **b,** Microscope image of droplets with a fueled PAA interfacial assembly. **c,** Counts of microfluidic oil-in-water droplets over time, with interfaces fueled by different EDC concentrations. Time 0 is when EDC

and PAA are mixed. **d,** Counts of microfluidic oil-in-water droplets over time, with EDC added at 0, 40, 80, and 120 minutes. Arrows show additions of 10 mM (blue) and 7.5 mM (yellow) EDC.

Outlook

Structuring liquids with programmable transience using fuel-driven interfacial assemblies offers access to all-liquid chemical systems with properties and compositions defined over space and time. To reach the full potential of these systems, expanding the range of times available for sustained assembly will be key, as will the use of functional materials beyond PAA to allow for dynamic functionalization of liquid compartment walls. These more versatile temporally and spatially controlled liquid systems offer exciting future possibilities for timed release, chemical reactions with autonomous mixing of components, or membranes with adaptive permeability and strength.

Data and materials availability

All data supporting the findings of this study are available within the Article, its Supplementary Information and Supplementary Files. Data are also available from the corresponding authors upon reasonable request.

References

1   Hyman, A. A., Weber, C. A. & Jülicher, F. Liquid-Liquid Phase Separation in Biology. *Annual Review of Cell and Developmental Biology* **30**, 39-58, doi:10.1146/annurev-cellbio-100913-013325 (2014).
2   Banani, S. F., Lee, H. O., Hyman, A. A. & Rosen, M. K. Biomolecular condensates:

organizers of cellular biochemistry. *Nature Reviews Molecular Cell Biology* **18**, 285-298, doi:10.1038/nrm.2017.7 (2017).

3   Cui, M., Emrick, T. & Russell, T. P. Stabilizing Liquid Drops in Nonequilibrium Shapes by the Interfacial Jamming of Nanoparticles. *Science* **342**, 460-463, doi:doi:10.1126/science.1242852 (2013).

4   Huang, C. *et al.* Bicontinuous structured liquids with sub-micrometre domains using nanoparticle surfactants. *Nature Nanotechnology* **12**, 1060-1063, doi:10.1038/nnano.2017.182 (2017).

5   Zhang, M. *et al.* Compartmentalized Droplets for Continuous Flow Liquid–Liquid Interface Catalysis. *Journal of the American Chemical Society* **138**, 10173-10183, doi:10.1021/jacs.6b04265 (2016).

6   Yan, J. *et al.* Structured-Liquid Batteries. *Journal of the American Chemical Society* **144**, 3979-3988, doi:10.1021/jacs.1c12417 (2022).

7   Feng, W. *et al.* Harnessing liquid-in-liquid printing and micropatterned substrates to fabricate 3-dimensional all-liquid fluidic devices. *Nat Commun* **10**, 1095, doi:10.1038/s41467-019-09042-y (2019).

8   Xie, G. *et al.* Compartmentalized, All-Aqueous Flow-Through-Coordinated Reaction Systems. *Chem* **5**, 2678-2690, doi:https://doi.org/10.1016/j.chempr.2019.07.016 (2019).

9   Herzig, E. M., White, K. A., Schofield, A. B., Poon, W. C. K. & Clegg, P. S. Bicontinuous emulsions stabilized solely by colloidal particles. *Nature Materials* **6**, 966-971, doi:10.1038/nmat2055 (2007).

10   Huang, C. *et al.* Structured Liquids with pH-Triggered Reconfigurability. *Advanced Materials* **28**, 6612-6618, doi:https://doi.org/10.1002/adma.201600691 (2016).

11   Sun, H., Li, L., Russell, T. P. & Shi, S. Photoresponsive Structured Liquids Enabled by Molecular Recognition at Liquid-Liquid Interfaces. *J Am Chem Soc* **142**, 8591-8595, doi:10.1021/jacs.0c02555 (2020).

12   Li, L. *et al.* Gated Molecular Diffusion at Liquid–Liquid Interfaces. *Angewandte Chemie International Edition* **60**, 17394-17397, doi:https://doi.org/10.1002/anie.202105500 (2021).

13   Zheng, Y. *et al.* Interfacial assembly of dendritic microcapsules with host–guest chemistry. *Nature Communications* **5**, 5772, doi:10.1038/ncomms6772 (2014).

14   Sun, H. *et al.* Redox-Responsive, Reconfigurable All-Liquid Constructs. *Journal of the American Chemical Society* **143**, 3719-3722, doi:10.1021/jacs.1c00429 (2021).

15   Zarzar, L. D. *et al.* Dynamically reconfigurable complex emulsions via tunable interfacial tensions. *Nature* **518**, 520-524, doi:10.1038/nature14168 (2015).

16   Boekhoven, J., Hendriksen, W. E., Koper, G. J. M., Eelkema, R. & Esch, J. H. v. Transient assembly of active materials fueled by a chemical reaction. *Science* **349**, 1075-1079, doi:doi:10.1126/science.aac6103 (2015).

17   Ragazzon, G. & Prins, L. J. Energy consumption in chemical fuel-driven self-assembly. *Nature Nanotechnology* **13**, 882-889, doi:10.1038/s41565-018-0250-8 (2018).

18   De, S. & Klajn, R. Dissipative Self-Assembly Driven by the Consumption of Chemical Fuels. *Advanced Materials* **30**, 1706750, doi:https://doi.org/10.1002/adma.201706750 (2018).

19   Boekhoven, J. *et al.* Dissipative Self-Assembly of a Molecular Gelator by Using a Chemical Fuel. *Angewandte Chemie-International Edition* **49**, 4825-4828, doi:10.1002/anie.201001511 (2010).

20   Bal, S., Das, K., Ahmed, S. & Das, D. Chemically Fueled Dissipative Self-Assembly that Exploits Cooperative Catalysis. *Angewandte Chemie International Edition* **58**, 244-247, doi:https://doi.org/10.1002/anie.201811749 (2019).

21   van Ravensteijn, B. G. P., Hendriksen, W. E., Eelkema, R., van Esch, J. H. & Kegel, W. K. Fuel-Mediated Transient Clustering of Colloidal Building Blocks. *Journal of the American Chemical Society* **139**, 9763-9766, doi:10.1021/jacs.7b03263 (2017).

22   Cheng, G. & Perez-Mercader, J. Dissipative Self-Assembly of Dynamic Multicompartmentalized Microsystems with Light-Responsive Behaviors. *Chem* **6**, 1160-1171, doi:https://doi.org/10.1016/j.chempr.2020.02.009 (2020).

23   Bian, T. *et al.* Electrostatic co-assembly of nanoparticles with oppositely charged small molecules into static and dynamic superstructures. *Nature Chemistry* **13**, 940-949, doi:10.1038/s41557-021-00752-9 (2021).

24   Ghosh, A., Paul, I. & Schmittel, M. Multitasking with Chemical Fuel: Dissipative Formation of a Pseudorotaxane Rotor from Five Distinct Components. *Journal of the American Chemical Society* **143**, 5319-5323, doi:10.1021/jacs.1c01948 (2021).

25   Wilson, M. R. *et al.* An autonomous chemically fuelled small-molecule motor. *Nature* **534**, 235-240, doi:10.1038/nature18013 (2016).

26   Tena-Solsona, M. *et al.* Non-equilibrium dissipative supramolecular materials with a tunable lifetime. *Nature Communications* **8**, 15895, doi:10.1038/ncomms15895 (2017).

27   Dhiman, S., Jalani, K. & George, S. J. Redox-Mediated, Transient Supramolecular Charge- Transfer Gel and Ink. *ACS Appl Mater Interfaces* **12**, 5259-5264, doi:10.1021/acsami.9b17481 (2020).

28   Hao, X., Chen, L., Sang, W. & Yan, Q. Periodically Self-Pulsating Microcapsule as Programmed Microseparator via ATP-Regulated Energy Dissipation. *Adv Sci (Weinh)* **5**, 1700591, doi:10.1002/advs.201700591 (2018).

29   Wanzke, C., Tena-Solsona, M., Rieß, B., Tebcharani, L. & Boekhoven, J. Active droplets in a hydrogel release drugs with a constant and tunable rate. *Materials Horizons* **7**, 1397-1403, doi:10.1039/C9MH01822K (2020).

30   Maiti, S., Fortunati, I., Ferrante, C., Scrimin, P. & Prins, L. J. Dissipative self-assembly of vesicular nanoreactors. *Nat Chem* **8**, 725-731, doi:10.1038/nchem.2511 (2016).

31   Lang, X. *et al.* Chemical fuel-driven transient polymeric micelle nanoreactors toward reversible trapping and reaction acceleration. *Chemical Communications* **57**, 5786-5789, doi:10.1039/D1CC00726B (2021).

32   Forth, J. *et al.* Building Reconfigurable Devices Using Complex Liquid–Fluid Interfaces. *Advanced Materials* **31**, 1806370, doi:https://doi.org/10.1002/adma.201806370 (2019).

33   Hossain, M. M., Atkinson, J. L. & Hartley, C. S. Dissipative Assembly of Macrocycles Comprising Multiple Transient Bonds. *Angewandte Chemie International Edition* **59**, 13807-13813, doi:https://doi.org/10.1002/anie.202001523 (2020).

34   Heckel, J., Loescher, S., Mathers, R. T. & Walther, A. Chemically Fueled Volume Phase Transition of Polyacid Microgels. *Angewandte Chemie International Edition* **60**, 7117-7125, doi:https://doi.org/10.1002/anie.202014417 (2021).

Acknowledgments

Author contributions

B.A.H. and S.E.G. designed and B.A.H. directed the study. B.A.H. and S.E.G. wrote the manuscript. S.E.G. conducted the experiments. T.P.R. and P.D.A. directed tensiometry and rheology experiments. All co-authors participated in data analysis and interpretation.

Competing interests

The authors declare no competing interests.

Supplementary Information:

Materials and Methods

Supplementary Figures 1–5

Supplementary Video 1